Winter-Dominated Little Ice Age Cooling in the Northern Gulf of Mexico Determined from Mg/Ca in Planktonic Foraminifera

by

Rita Marie Crouch

A thesis submitted in partial fulfillment of the requirements for the degree of
Master of Science,
Department of Environmental Science and Policy
College of Arts and Sciences
University of South Florida St. Petersburg

Co-Major Professor: Joseph M. Smoak, Ph.D.
Co-Major Professor: Richard Z. Poore, Ph.D.
Armando Hoare, Ph.D.

Date of Approval:

March 31, 2014

Keywords: *Globigerinoides ruber* (pink and white varieties), *Globorotalia truncatulinoides* (non-encrusted variety), seasonality, Late Holocene, paleogeology

DEDICATION

I dedicate this work to my deceased father, Richard Glenn Beckhorn. Knowing he is looking down on me has inspired me to keep going to make him proud. Also to my mother, Rita Anne Beckhorn, sister, Michelle Beckhorn, and most of all to my husband, Clay Crouch: I thank you endlessly for all of the support, love, and encouragement you have given me throughout my graduate career. I could not have done it without you.

TABLE OF CONTENTS

LIST OF TABLES

LIST OF FIGURES

ABSTRACT

Reconstructing late Holocene sea-surface temperature (SST) establishes a baseline for preindustrial climate change, which has important applications for climate models and forecasts to predict current anthropogenic influences. The Medieval Warm Period (MWP) (~900 to 1300 AD) and Little Ice Age (LIA) (~1400 to 1800 AD) are the two most recent preindustrial climate change extremes. Mean-annual SST changes in the northern Gulf of Mexico (GOM) during this time period are well known, but the seasonal distribution of these changes are not. This study presents the first paired record showing seasonal distribution of temperature changes over the past millennium in the northern GOM. Mg/Ca derived from planktonic foraminifera species *Globigerinoides ruber* (white and pink varieties) and *Globorotalia truncatulinoides* (non-encrusted) yield a record of mean-seasonal (winter and summer) and mean-annual sea-surface temperature (SST) from the northern GOM. During the MWP, all three records of mean-annual and mean-seasonal (winter and summer) SST were within error of modern observed SSTs, with a difference between summer and winter SSTs of ~3ºC. During the LIA, the difference between summer and winter SSTs was large (~8ºC), with mean-winter and mean-annual SST consistently colder than modern observed SSTs. The data presented clearly show muted summer SST changes coupled with enhanced winter and mean-annual SST changes during the LIA, indicating that winter seasonality drove the observed mean-annual record and dominated the observed LIA cooling in the northern GOM. These results also indicate that enhanced winter seasonality plays an important role in the climate of the GOM region.

INTRODUCTION

The Medieval Warm Period (MWP) (~900 to 1300 AD) and Little Ice Age (LIA) (~1400 to 1800 AD) are the two most recent preindustrial climate change extremes. During the MWP, many regions exhibited temperature excursions that were as warm as, if not warmer than, modern times (e.g., Bradley et al., 2003). During the LIA, many regions exhibited colder than modern temperature excursions; it was one of the coldest time periods since the Last Glacial Maximum ~20,000 years ago (e.g., Lamb, 1995). While effects of the MWP and LIA have been reported throughout the globe, they significantly vary by region and proxy type. Furthermore, seasonality of temperature changes during this climatically important time period is not well understood. Regional reconstructions of seasonal sea-surface temperature (SST) can potentially reveal important influences on seasonal variability and natural forcing mechanisms, provide insight into modern climate change, and improve climate models and forecasts (Jones et al., 2001; Cane, 2010).

There is evidence that the MWP and LIA may have been global climate extremes. (e.g. Broecker, 2001). Ice core studies based on stable isotope ratio data from the Antarctic Ross Sea region in the southern hemisphere determined that air temperatures warmed and cooled concurrently with the northern hemisphere during the MWP and LIA (Kreutz et al., 1997; Bertler et al., 2011). Bertler et al. (2011) determined air temperatures were ~0.35°C warmer during the MWP and ~2°C cooler during the LIA in the McMurdo Dry Valleys compared to modern times. This evidence contradicts the bipolar see-saw

hypothesis, which would predict asynchronous climate change between the northern and southern hemispheres, and indicates that MWP and LIA climate changes were likely linked to a ubiquitous global-forcing mechanism (Kreutz et al., 1997; Broecker, 2001; Bertler et al. 2011).

Although evidence shows the MWP and LIA as global events, they significantly vary in timing and extent depending on location and proxy type (Table 1). Recent records in low-latitude regions show the MWP and LIA climate extremes during similar time periods, with MWP SSTs similar to observed modern SSTs (e.g., Newton et al., 2006; Richey et al., 2007). However, the extent of LIA cooling significantly varies. For example, based on Mg/Ca in planktonic foraminifera, Richey et al. (2007) found LIA cooling to be ~2 to 3ºC in the northern GOM, while deMenocal et al. (2000) found it to be ~3 to 4ºC based on faunal analysis off of the west coast of Africa.

Recent studies in low-latitude regions have also revealed unusually large temperature fluctuations over the past millennium in comparison to composite mean-hemispheric temperature reconstructions that suggest a <0.5ºC change (e.g., Mann et al., 2009). However informative, hemispheric studies systematically remove low frequency regional changes due to data processing techniques. Researching regional changes in temperature leads to better understanding of past climate change and potential natural sources influencing the region.

Currently, there are several records of mean-annual SST changes over the past millennium in the GOM region. Richey et al. (2007) determined a ~3°C range between maxima and minima mean-annual SSTs over the past 1400 years in the northern Gulf of Mexico (GOM), which corresponds to 75% of the glacial-interglacial range in this region.

While few SST reconstructions in the GOM region extend back into the MWP, Richey et al. (2007) also showed mean-annual SST was within error of modern temperatures based on Mg/Ca in planktonic foraminifera. Multiple proxy-based foraminiferal and coral SST records in this region showed SST cooling of ~2 to 3°C during the LIA (Winter et al., 2000; Watanabe et al., 2001; Black et al., 2007; Kilbourne et al., 2008; Richey et al., 2009). Richey et al. (2009) suggested that a reduced Atlantic Warm Pool (AWP) linked to sunspot minima and associated positive feedbacks caused the dramatic LIA cooling of this region. However, solar forcing alone can only explain SST excursions of <1°C, suggesting other forcing mechanisms at work (Richey et al., 2009).

Previous studies have not investigated the seasonality of SST variability within this climatically important time period in the GOM, missing potentially important influences of seasonal variability. The goal of this study is to determine whether or not SST variability in the GOM region is seasonally biased. Here we present the first paired records of mean-annual and mean-seasonal (winter and summer) SST in the northern GOM that extend through the last 1000 years, capturing the MWP and LIA.

Regional setting

The GOM is greatly influenced by the Loop Current and Atlantic Warm Pool (AWP). The Loop Current is the main current in the GOM and carries warm waters up from the Caribbean Sea through the Yucatan Strait into the GOM, then leaves through the Florida Straits into the North Atlantic Ocean (Poore et al., 2004). The AWP is comprised of GOM, Caribbean Sea, and western tropical North Atlantic waters warmer than 28.5°C (Wang and Enfield, 2001; Wang et al., 2006). The AWP significantly varies in size, extent, and SST, both seasonally and inter-annually on multidecadal time scales (Wang et

al., 2006). During boreal summer, the AWP reaches its maximum size and extent by expanding through the GOM along with deeper Loop Current penetration into western and northern GOM and northward migration of the Intertropical Convergence Zone (ITCZ) (Wang and Enfield, 2003; Poore et al., 2004). During boreal winter the AWP disappears, the Loop Current does not extend into western and northern GOM, and the ITCZ lies near the equator (Wang and Enfield, 2003; Poore et al., 2004). The AWP is greatly influenced by ocean-atmosphere dynamics such as the El Niño-Southern Oscillation, the North Atlantic Oscillation, the Atlantic Multidecadal Oscillation, and migration of the ITCZ (Poore et al., 2004). The AWP is also a major moisture source to the North American continent (Wang et al., 2008; Wang et al., 2011).

During boreal summer, the AWP and Loop Current are the main sources of warm waters in the northern GOM. The SST can also be uniform throughout the GOM during the summer months (Dowsett et al., 2003). During boreal winter, the AWP is minimal in extent, and the Loop Current generally does not penetrate in the northern GOM; however, variations can have potential affects on winter seasonality in the northern GOM (Poore, 2008).

Planktonic foraminifera

Mg/Ca as a proxy for sea-surface temperature (SST)

Planktonic foraminifera are single-celled eukaryotes ideal for SST reconstructions. They are a primary contributor of biogenic calcite to marine sediments due to their high abundance and short life cycles of approximately two to four weeks (Spero, 2001). The chemical composition of planktonic foraminiferal tests is ~99% calcium carbonate. However, as ocean SST increases, the minor element Magnesium

(Mg) substitutes for Calcium (Ca); thus, the amount of Mg substituted for Ca is a function of temperature (Chave, 1954; Wefer et al., 1999; Dowsett, 2007). Anand et al (2003) determined that for every 1°C increase in temperature, Mg/Ca increases 9%. Therefore, Mg/Ca in calcite tests of planktonic foraminifera can serve as a SST proxy (Dekens et al., 2002; Anand et al., 2003).

Seasonal habitat of Globigerinoides ruber (pink and white varieties)

The tropical to subtropical planktonic foraminifera species, *Globigerinoides ruber* (pink and white varieties), is a reliable recorder of past oceanic conditions and is commonly used as a proxy for SST reconstructions (Dekens et al. 2002; Anand et al., 2003). A global study of 20 sediment trap samples determined optimum SST ranges for *G. ruber,* pink and white, separately, as 23 to 30°C and 22 to 31°C, respectively (Žarić et al., 2005), with a salinity tolerance range of 22 to 49 psu (Bijma et al., 1990; Ferguson et al., 2008). Plankton tow data from the subtropical Sargasso Sea show that the highest concentrations of *G. ruber* (pink and white) are found between 23 and 27°C (Bé and Hamlin, 1967; Tolderlund and Bé, 1971).

Photoautotrophic dinoflagellate symbionts confine *G. ruber* (pink and white) to the euphotic zone of the ocean. Plankton tow data from the Sargasso Sea show that *G. ruber* is most abundant in the upper 10 m of the water column (Bé and Hamlin, 1967). Calcification depths estimated from $\delta^{18}O_{calcite}$ formed in equilibrium with seawater revealed depths of 0 to 50 m for *G. ruber* (white) and 0 to 25 m for *G. ruber* (pink) (Anand et al., 2003). Furthermore, plankton tow studies from the Western North Atlantic show distinct differences in seasonal fluxes between *G. ruber* (pink and white), where *G.*

ruber (pink) is most abundant in summer months and absent during colder months (Bé and Hamlin, 1967; Tolderlund and Bé 1971; Deuser and Ross, 1989).

Five years of weekly resolution sediment trap data from the GOM (25.7°N latitude and 90.3°W longitude) (see Figure 3) show seasonal fluxes in *G. ruber* (pink and white) consistent with Sargasso Sea data. *G. ruber* (pink) maximum fluxes occur between April-October and are nearly non-existent during the colder months of December-March, while *G. ruber* (white) occurs year-round (Reynolds et al., 2013; Richey et al., 2012; Figure 1). Because *G. ruber* (white) precipitate year-round in the GOM, *G. ruber* (white) may be interpreted as a mean-annual signal. Several studies have already done so with success (see Table 3). Because *G. ruber* (pink) precipitate mainly during the warmer months, *G. ruber* (pink) may be interpreted as a mean-summer signal.

Seasonal habitat of Globorotalia truncatulinoides (non-encrusted)

The subtropical species, *Globorotalia truncatulinoides*, exhibits two distinct test morphologies with significant offsets in shell chemistry related to depth: one with a primary calcite layer (non-encrusted) and one with a secondary calcite layer (encrusted) (McKenna and Prell, 2004). Plankton tow studies suggest depth differences are due to complex migration related to reproduction, where juveniles ascend to the euphotic zone to secrete a primary calcite layer and mature before sinking down into colder, deeper waters to secrete a secondary calcite layer and reproduce (Hemleben et al., 1985). Based on plankton tow data from the Sargasso Sea, the non-encrusted tests are produced in the upper 200 m of the water column, and represent specimens that were eaten or otherwise died without reproducing. Prior to reproduction, the shell encrustation occurs in depths deeper than 800 m (Hemleben et al., 1985). In the Western North Atlantic, plankton tow

data show *Gl. truncatulinoides* is found in surface temperatures ranging from 10.5 to 28.1°C with optimum temperatures between 15.2°C and 22.0°C, and a salinity tolerance of 35.75 to 36.63 psu (Tolderlund and Be, 1971). Plankton tow data show *Gl. truncatulinoides* abundance peaks in December in the subtropical Sargasso Sea, and in January off the coast of Bermuda, when the water is well mixed and deep convection is greatest (Tolderlund and Be, 1971; Hemleben et al., 1985).

In the GOM, the *Gl. truncatulinoides* population peaks in winter months as well, with 90% of the flux occurring in January and February (Spear et al., 2011; Figure 2). Based on Mg/Ca and $\delta^{18}O$ analyses, Spear et al. (2011) determined significant offsets between the shell chemistry of *Gl. truncatulinoides* non-encrusted and encrusted tests in the GOM: the encrusted tests calcify in deep, cold waters whereas the non-encrusted tests calcify within the winter surface-mixed layer (no deeper than 120±14 m). The fact that 90% of *Gl. truncatulinoides* (non-encrusted) precipitates during January and February, coupled with the fact that the non-encrusted tests precipitate within the surface-mixed layer, reveals the strong potential of *Gl. truncatulinoides* (non-encrusted) as a proxy for winter SST in the GOM.

METHODS

Study location

The Fisk Basin is located on the continental slope in the northern GOM approximately 250 km from the modern Mississippi River delta (Figure 3). High sedimentation rates (20 to 40 cm/kyr) due to terrigenous input from Mississippi River transport, allow for high multidecadal resolution (Richey et al., 2009). Minimal calcite dissolution, documented by the presence of aragonitic benthic foraminifers and pteropod shells, indicates good preservation of planktonic foraminifers down-core. Furthermore, the calcite compensation depth (CCD) in the Atlantic Ocean, defined as the depth at which dissolution rate is higher than the calcium carbonate accumulation rate, is well below the Fisk Basin depth at approximately 4-5 km (Pinet, 2009). The 35.5 cm long boxcore, 2010-FB1-BC1, was extracted at 27°33.0N, 92°10.1W, from 817 m water depth by U.S. Geological Survey researchers on the *R/V Cape Hatterras* during a cruise in the Spring of 2010.

Age model

The age model for boxcore 2010 FB1-BC1 is based on five accelerator mass spectrometry (AMS) ^{14}C dates based on mixed planktonic foraminifers (Table 2). Samples were processed at the ^{14}C laboratory of the U.S. Geological Survey in Reston, Virginia and analyzed at the Center for Accelerator Mass Spectrometry, Lawrence Livermore National Laboratory in Livermore, California. ^{14}C dates were calibrated to calendar years using the MARINE09 ^{14}C calibration data set (Figure 4) (Reimer et al.,

2009). The calibrated age model shows a linear sedimentation rate of 18.9 cm/kyr (R^2=0.99) with an age resolution of 26.5 years per half-centimeter sample.

Sediment sampling and processing

Core 2010-FB1-BC1 was extruded at 5mm increments and freeze-dried. Samples were placed in beakers filled with tap water and Calgon© solution, and placed on a shaker plate for one hour in order to break up clays and muds. Samples were then washed over a 63 μm sieve for 5 to 20 minutes. Once fine grain material was removed, samples were dried, weighed, and sieved over 150 μm.

G. ruber (pink and white varieties, separately) and *Gl. truncatulinoides* (non-encrusted) were picked from the 250 to 355 μm and 300 to 500 μm size fractions, respectively. Only pristine foraminifers with whole tests were included. Ideally, at least 60 foraminifers are picked for analysis; but due to low foraminiferal abundance in some intervals, a minimum of 20 individuals for *G. ruber* (pink and white varieties) and 10 individuals for *Gl. truncatulinoides* (non-encrusted) was allowable.

Stable isotope and Mg/Ca analyses

Once picked, samples were sonicated in methanol for 5 seconds to remove particles from within tests. Samples were then allocated for Mg/Ca and $\delta^{18}O$ analysis based on the number of individuals. Due to low abundance of non-encrusted *Gl. truncatulinoides* in all samples, only Mg/Ca analyses were performed. For *G. ruber* (pink and white), only Mg/Ca analyses were performed on samples with fewer than 20 individuals. Samples with 20 to 60 individuals were crushed for Mg/Ca analyses, while taking a ~50 to 80 μg aliquot for isotopic analyses. Samples with 60 or more individuals were evenly divided for both Mg/Ca and $\delta^{18}O$ analyses. Half of each sample was gently

crushed between two glass plates for Mg/Ca analyses, while the other half was pulverized and homogenized for $\delta^{18}O$ analyses. Samples with 90 or more individuals were separated into different aliquots for replicate analysis to assess cleaning proficiency and analytical error. $\delta^{18}O$ analyses were performed on a ThermoFinnigan Delta Plus XL dual-inlet mass spectrometer at the Analytical Laboratory for Paleoclimate Studies at the Jackson School of Geosciences, University of Texas in Austin, Texas.

Foraminiferal trace metal cleaning steps followed protocols suggested by Barker et al. (2003). Clay particles were brought into suspension during milliQ water and methanol rinses, and siphoned off after foraminifer tests settled on the bottom of a microcentrifuge tube. Organic matter was removed through oxidation using a heated buffered peroxide solution for 10 minutes. Any remaining adsorbed contaminants were removed through a weak acid (0.001N HNO_3) leach. Lastly, samples were dissolved in 0.075 HNO_3 immediately before Mg/Ca analysis on a Perkin Elmer Optima 7300 dual-view inductive coupled plasma-optical emission spectrometer (ICP-OES) at the U.S. Geological Survey, St. Petersburg Coastal Marine Science Center in Saint Petersburg, FL.

Sea-surface temperature (SST) estimates

SSTs were calculated using the Anand et al. (2003) calibration equations:

$Mg/Ca = [0.449 \times \exp(0.09 \cdot SST)]$ – *G. ruber* (white)

$Mg/Ca = [0.381 \times \exp(0.09 \cdot SST)]$ – *G. ruber* (pink)

$Mg/Ca = [0.359 \times \exp(0.09 \cdot SST)]$ – *Gl. truncatulinoides*

The species-specific equations are based on Mg/Ca data from 6 years of sediment trap material from the Sargasso Sea combined with a long time series of hydrographic data (April 1978 through May 1984; temperature and salinity 0 to 2600 m).

While temperature is the main control on Mg uptake, salinity may be a secondary controlling factor, thus skewing calibrated SST values. For example, a culturing study of *G. sacculifer* found that a 10 psu salinity increase also increased Mg/Ca values by 110% (equivalent to ~8°C change), while changes less than 3 psu had no affect on Mg uptake (Nürnberg et al., 1996). A recent culturing study of *G. ruber* (white) showed that Mg/Ca values increase 5±3% per psu increase in salinity, while *G. ruber* (white) core-top measurements show a significantly higher dependence of 27±4% (Kisakürek et al., 2008; Arbuszewski et al., 2010). Currently, there is no evidence that salinity affects Mg/Ca values at salinities less than 35 psu (Arbuszewski et al., 2010). Since the average salinity of the GOM is 35 psu, with a seasonal range of 34 to 36 psu, salinity is likely a minimal controlling factor on Mg uptake in the GOM (Levitus, 2003).

Existing calibration equations are not specific to the hydrologic conditions of the northern GOM; therefore the calibration and validation step is very important to reduce uncertainty in the results. However, previous studies in the GOM have used these equations with success (LoDico et al., 2006; Nürnberg et al., 2008; Richey et al., 2009; Williams et al., 2010; Spear et al., 2011; Richey e al., 2011; Richey et al., 2012), including a study from within the Fisk basin (Richey et al., 2007). For example, with 17 replicates for *G. ruber* (pink) and 13 replicates for *G. ruber* (white), both with more than 60 individuals in each sample, Richey et al. (2012) calculated core-top temperatures that corresponded to modern summer (27°C) and mean annual (25.4°C) SST (Table 3).

RESULTS

Mg/Ca data

Mg/Ca instrumental precision was 0.36% root-mean standard deviation based on a calibrated ICP-OES solution. The average analytical precision for *G. ruber* (pink) Mg/Ca was ±0.10 mmol/mol based on 56% replicate sample measurements (n=23), and ±0.14 mmol/mol based on 44% replicate sample measurements for *G. ruber* (white) (n=18). Due to extremely low *Gl. truncatulinoides* (non-encrusted) abundance, no Mg/Ca replicate measurements were made. Mean core-top Mg/Ca values for *G. ruber* (white) and *G. ruber* (pink) were 3.98 (±0.16) and 3.96 (±0.09) mmol/mol, respectively (Figure 5a, 5b). For *Gl. truncatulinoides* (non-encrusted), the core-top value was 2.21 mmol/mol (Figure 5c).

Mean-seasonal (winter and summer) and mean-annual calculated SSTs over the past millennium, based on Mg/Ca data, are provided in Figure 6. The main features of the paired records include a distinct shift from warmer to cooler SSTs and from low to high SST variability coupled with large divergences between the mean-seasonal and mean-annual SST records ca. 1250 CE. Average winter SST excursions are much larger than average summer SST changes; the total amplitude of SST variability, from maxima observed between 900 and 1300 CE and minima observed between 1600 and 1900 CE, is ~4°C for the average summer record and ~7°C for the average winter record. The average mean-annual SST range from maximum to minimum is ~7ºC, the same as the mean-

winter SST range. An overall cooling trend is seen in each SST record since 1250 CE, where winter SST cooling is more dramatic than summer.

$\delta^{18}O$ data

Paired Mg/Ca and $\delta^{18}O_{calcite}$ measurements are used to calculate the oxygen isotope composition of seawater ($\delta^{18}O_{seawater}$) which can reveal salinity changes in the record. Because SST estimates based on Mg/Ca measurements and $\delta^{18}O_{calcite}$ measurements come with uncertainties in absolute values, only $\delta^{18}O_{seawater}$ trends are illustrated. Raw *G. ruber* (white) $\delta^{18}O_{calcite}$ show an overall trend toward more positive values from ca. 900 to 1700 CE, followed by a large abrupt shift (~1.00 VPDB) towards more negative values ca. 1750 to 1810 CE (Figure 7a). In comparison, raw *G. ruber* (pink) $\delta^{18}O_{calcite}$ exhibit relative stability over the past millennium except for a similar but smaller shift (~0.70 VPDB) ca. 1675 to 1850 CE (Figure 7b). *Gl. truncatulinoides* (non-encrusted) $\delta^{18}O_{calcite}$ were not analyzed due to lack of material. The main features of the *G. ruber* (white) $\delta^{18}O_{seawater}$ are two maxima centered around 1400 to 1500 CE and 1750 CE representing periods of increased salinity (Figure 8a). *G. ruber* (pink) $\delta^{18}O_{seawater}$ show a shift to decreased salinity ~1700 CE (Figure 8b).

DISCUSSION

Seasonality of the MWP and LIA in the northern GOM

The MWP and LIA occurred between 900-1250 and 1250-1850 CE, respectively. The MWP may have begun earlier, but interpretations are limited to the time frame of this study. The MWP exhibited relatively constant and sustained warm sea-surface temperatures (SSTs) in all three records until 1250 CE when SST variability significantly increased (Figure 6). The LIA consisted of a dramatic drop in both mean-winter and mean-annual SSTs, while mean-summer SSTs dropped slightly in comparison. The paired records of mean-seasonal (summer and winter) and mean-annual SST show that the northern GOM exhibited high winter SST variability coupled with muted summer SST changes during the LIA. The records also suggest that winter variability essentially drove the observed mean-annual SST changes during the LIA in the northern GOM.

The magnitude of change between summer and winter SST ($\Delta T_{summer\text{-}winter}$) is shown in Figure 9. During the MWP, the $\Delta T_{summer\text{-}winter}$ range was ~3ºC, which is 2ºC smaller compared to modern (~5ºC). During the LIA, the $\Delta T_{summer\text{-}winter}$ range was ~8ºC, which is much larger than both the MWP range and modern $\Delta T_{summer\text{-}winter}$. After the LIA, $\Delta T_{summer\text{-}winter}$ remains larger than that of the MWP. These results show that enhanced seasonality, defined by colder winters, dominated the LIA time period and has continued into the present.

GOM regional comparison

Previously reconstructed GOM records are mostly mean-annual weighted SST records; therefore, seasonal comparisons are extremely limited in this region. However, the mean-annual data presented here follow similar trends to other records in the region. SSTs based on *G. ruber* (white) Mg/Ca from the Fisk, Garrison, and Pigmy basins in the northern GOM (see Figure 3) show similar LIA cooling of ~3°C, with minima centered around 1750-1850 CE (Richey et al., 2007; 2009) (Figure 10). SSTs derived from sclerosponge Sr/Ca in Jamaica also show similar LIA cooling of ~3°C, with maximum cooling centered on 1700 CE (Haase-Schramm et al., 2003). Furthermore, SSTs based on Mg/Ca in the planktonic foraminifer *Globigerina bulloides* show a similar LIA cooling of ~2°C (Black et al., 2007; Richey et al., 2007).

While seasonal comparisons in the GOM region are extremely limited, a regional European study based on a compilation of both instrumental and proxy data representing seasonal and annual air temperature changes over the past ~500 years exhibited similar trends to our record (Luterbacher et al., 2004). The study determined winter seasonality as more variable with minima centered ca. 1700 CE, while summers showed insignificant variation. However, the degree of temperature changes was minimal compared to the GOM region, with winter cooling of 0.5°C and annual cooling of 0.25°C. This can be explained by the fact SST and air temperature changes are affected differently by natural variations in climate.

Global comparison

Global composite air temperature records show the MWP and LIA generally occurred around 900-1300 and 1400-1800 CE, which is within chronological uncertainty

of this study. However, the composite air temperature records show temperature excursions occurring on a much smaller scale, likely due to data processing techniques that remove regional low frequency temperature changes. Moberg et al. (2005) determined a temperature range of 0.65°C based on a multi-proxy approach on Northern hemisphere data. Mann et al. (2009) utilized a global multi-proxy compilation of data and determined temperatures ~0.2 °C warmer during the MWP and ~0.4°C cooler during the LIA, a change of ~0.6°C. Both studies attribute radiative forcing as the main driver of these temperatures changes. Because radiative forcing alone can only explain temperature excursions of <1ºC, additional factors must be influencing the GOM region.

Various factors attributed to MWP and LIA climate

The MWP and LIA may be attributed to extreme temperature anomalies occurring every ~1500±500 (Bond et al., 1997; deMenocal et al., 2000); however, this pattern has not been resolved on a global scale (Bond et al., 1997). While Crowley (2000) determined that solar forcing and volcanism explain 41-64% of preindustrial climate change, Bond et al. (2001) claimed that changes in surface winds and hydrography triggered by minor changes in solar irradiance can explain the temperature anomalies. Ruddiman (2007) attributed early anthropogenic forcing through actions such as deforestation and rice irrigation as the main driver for Holocene climate variability despite natural forcing mechanisms. Debate also revolves around the role of thermohaline circulation and whether it influenced MWP and LIA climate change (Broecker, 2001; Bertler et al., 2011). While these factors are all potential sources for the MWP and LIA climate events, regional as well as seasonal factors are also important to consider.

Richey et al. (2009) speculated that a reduced AWP was the main influence on the dramatic cooling evidenced in the GOM during the LIA. Since the AWP mainly develops during the summer without influencing winter SSTs, it is not a likely source for the dramatic cooling evidenced in this region. However, natural variations in the size and extent of the AWP could potentially influence our winter SST record.

Solar minima took place during the LIA roughly around the same time SST minima occurred in the GOM (Richey et al., 2009). It is possible that associated feedbacks, such as atmospheric circulation changes as a result of solar variation, could amplify cooling due to solar minima and explain the >1°C cooling in the region. For example, cooling in the northern hemisphere due to solar minima could result in migration of the ITCZ further south during the winter, allowing cold northerly winds to influence GOM winter SSTs. Further research is needed to better understand associated feedbacks that could affect the seasonality of the region.

CONCLUSION

This study showed the first paired records of mean seasonal (winter and summer) and mean-annual SST over the past thousand years in the northern GOM. Mg/Ca data measured from three planktic foraminifera species were used to obtain the paired records. *Globigerinoides ruber* (pink) represented summer SST, *Globigerinoides ruber* (white) represented mean-annual SST and *Globorotalia truncatulinoides* (non-encrusted) represented mean-winter SST. During the MWP (930 to 1250 CE), all three records showed SSTs within error of modern observed SSTs for their respective seasons. The MWP $\Delta T_{summer\text{-}winter}$ was also small (~3ºC) relative to modern $\Delta T_{summer\text{-}winter}$ (~5ºC). During the LIA (1250 to 1850 CE), mean-winter and mean-annual SSTs were consistently colder than modern observed SSTs while mean-summer SSTs were not. The LIA $\Delta T_{summer\text{-}winter}$ was large (~8°C) compared to modern. Enhanced seasonality, defined by colder winters, clearly dominated the LIA cooling in the northern GOM. The causes of these recent pre-industrial climate trends are still unknown. Teasing out seasonal signals from SST records during the MWP and LIA climate events can potentially improve climate modeling, reveal climatic influences associated with these events, and improve climate forecasts.

TABLES

Table 1: MWP and LIA regional variability

Study Location	Proxy	MWP (CE)	ΔT °C[1]	LIA (CE)	ΔT °C[2]	Source
Low-Latitude Regions						
Makassar Strait, Indonesia	Paired $\delta^{18}O$ and Mg/Ca foraminifera	1000-1400 1000-1250	+0 to +1 W.E.*	1400-1850 1550-1850	-1.5 -0.5 to -1	Newton et al. (2006) Oppo et al. (2009)
Northern Gulf of Mexico	Mg/Ca foraminifera	1000-1400	W.E.	1400-1850	-2 to -3	Richey et al. (2007, 2009)
West Africa	Faunal analysis	800-1200	+0 to +1	1300-1850	-3 to -4	deMenocal et al. (2000)
High-Latitude Regions						
Ross Sea, Antarctica	Ice core	1100-1300	+0.35	1300-1850	-2	Bertler et al. (2011)
High-latitude Europe	Proxy fusion of pollen and tree ring data	900-1200	+1.02 to +1.19	1300-1800	-1.14 to -1.39	Helama et al. (2010)
Western Central Asia	Tree ring data	900-1300	-0.07	1200-1850	-0.2	Esper et al. (2002)
Hemispheric Compilations						
Northern Hemisphere	Multi-proxy approach	950-1250	+0.2	1400-1700	-0.4	Mann et al. (2009)
Northern Hemisphere	Multi-proxy approach	N.D.**	+0.4	N.D.	-0.7	Moberg et al. (2005)

[1]Temperature change relative to modern temperatures during MWP
[2]Temperature change relative to modern temperatures during LIA
*Within error of modern temperatures
** Not defined in paper

Table 2: ^{14}C results for 2010 Fisk Basin boxcore

Sample ID	Material	Region	$\delta^{13}C$	^{14}C Age*	±	Calibrated Calendar Year**	Error
2010-FB1-BC1 0-0.5cm	forams	Gulf of Mexico	0.74	>Modern		1950	
2010-FB1-BC1 10.5-11cm	forams	Gulf of Mexico	0	900	30	1441	53
2010-FB1-BC1 20-20.5cm	forams	Gulf of Mexico	0	1380	30	1027	88
2010-FB1-BC1 28-28.5 cm	forams	Gulf of Mexico	0	1885	30	521	85
2010-FB1-BC1 34.5-35cm	forams	Gulf of Mexico	1.49	2245	30	103	93

*^{14}C dates are based on the Libby half-life of 5568 years

** Based on MARINE09 ^{14}C calibration data set using 2σ average age with a 1.0 probability.

Table 3: Core-top calibrations from GOM using Anand et al. (2003)

Mg/Ca (mmol/mol)	Mg/Ca-derived SST (°C)	*Observed seasonal SST (°C)	Source
***G. ruber* (white): Mean-Annual weighted SST**			
4.86	26.5	25.4	LoDico et al. (2006)
4.43	25.4	25.4	Richey et al. (2007, 2009, 2011)
4.31	25.2	25.4	Richey et al. (2012)
3.44	24.5	25.4	Nurnberg et al. (2008)
***G. ruber* (pink): Mean-Summer weighted SST**			
4.36	27.1	27	Richey et al. (2012)
***Gl. truncatulinoides* (non-encrusted): Mean-Winter weighted SST**			
2.93	22.7	22.2	Spear et al. (2011)

*Observed values are based on National Oceanographic Data Center World Ocean Atlas 1994

FIGURES

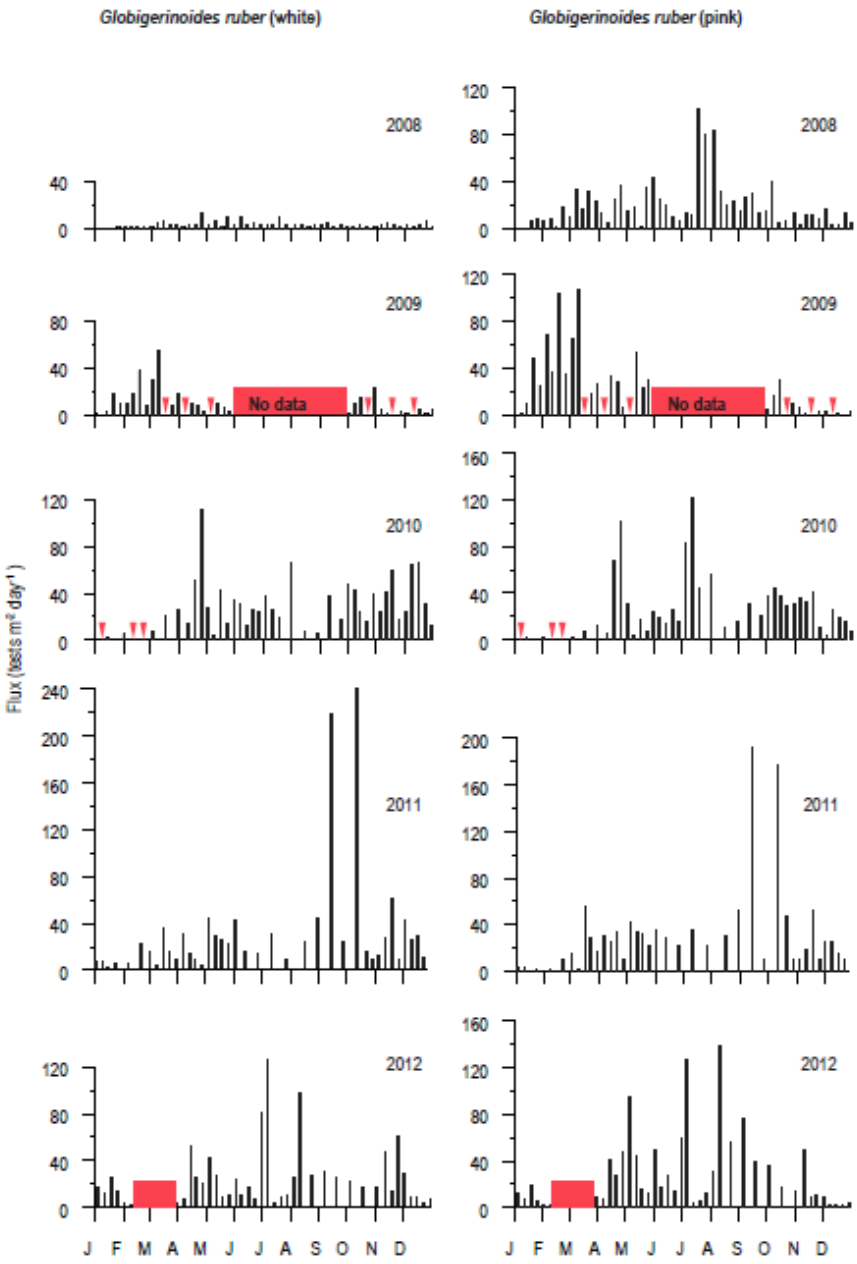

Figure 1: *Globigerinoides ruber* (white and pink) average flux data from the northern GOM from 2008 to 2012 (Reynolds et al., 2013).

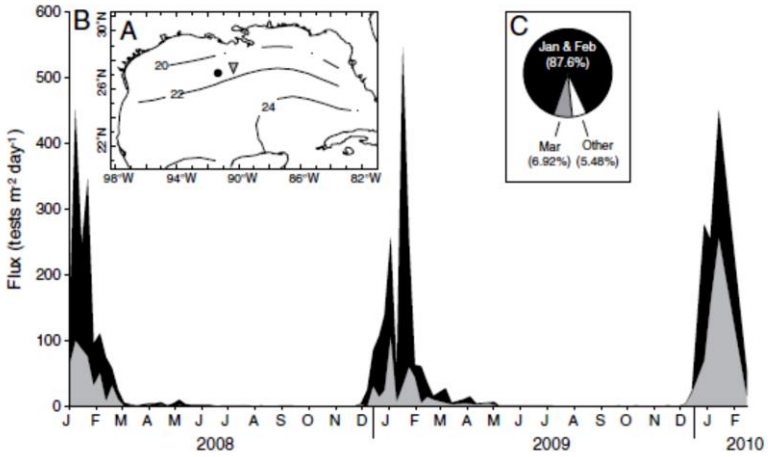

Figure 2: Flux of *Globorotalia truncatulinoides* encrusted (black shaded areas) and non-encrusted (gray shaded areas) in the northern GOM (Spear et al., 2011).

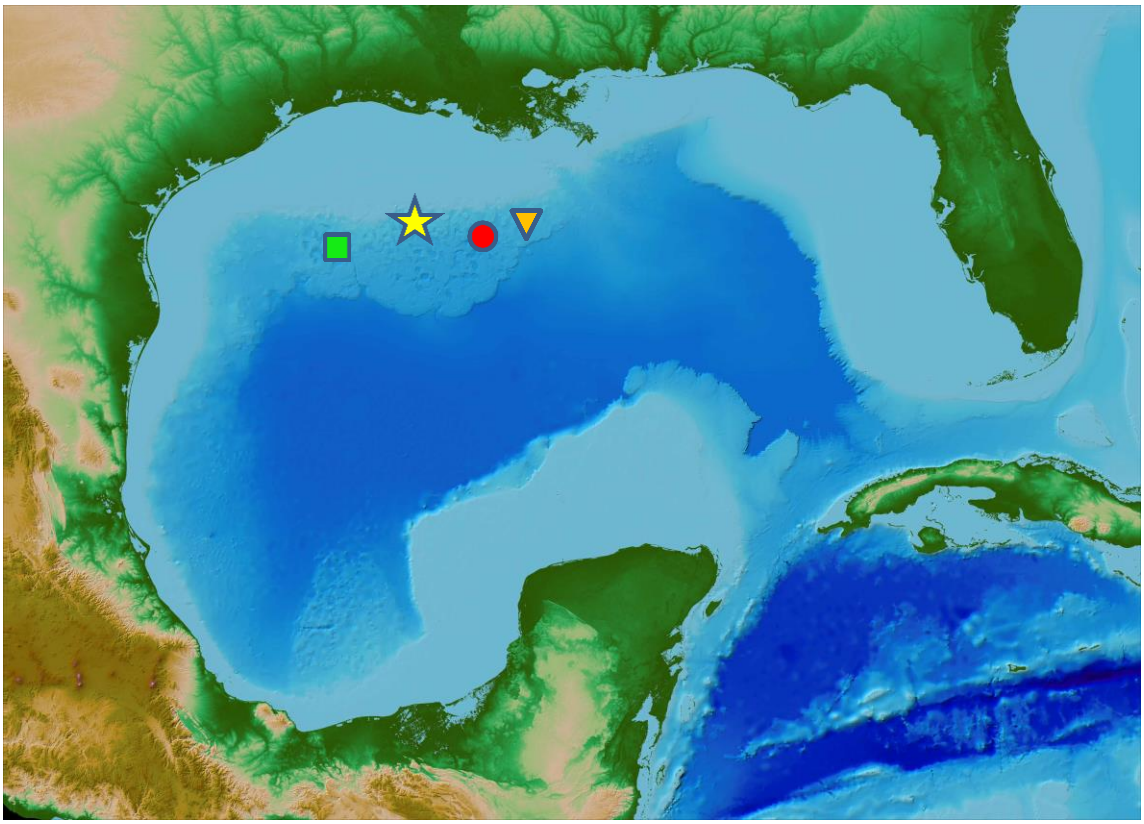

Figure 3: Locations of the Fisk Basin (this study; star), Garrison Basin (square), Pigmy Basin (circle), and the sediment trap mooring in the northern Gulf of Mexico (inverted triangle).

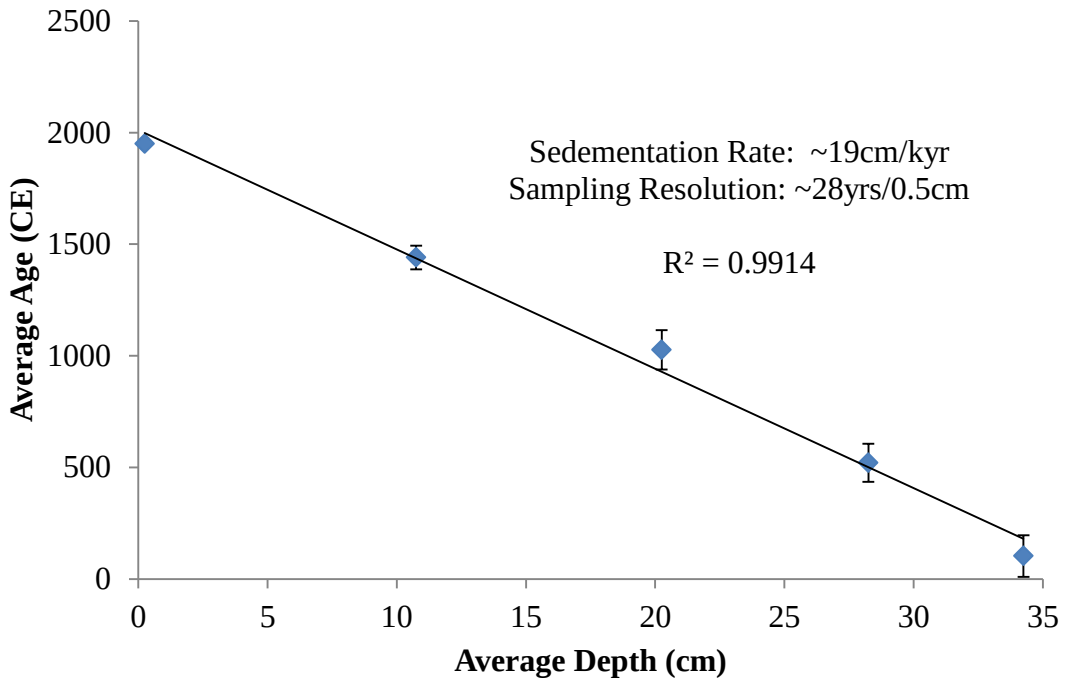

Figure 4: Age model for boxcore 2010 FB1-BC1 based on five accelerator mass spectrometry (AMS) ^{14}C dates that were based on mixed planktonic foraminifers.

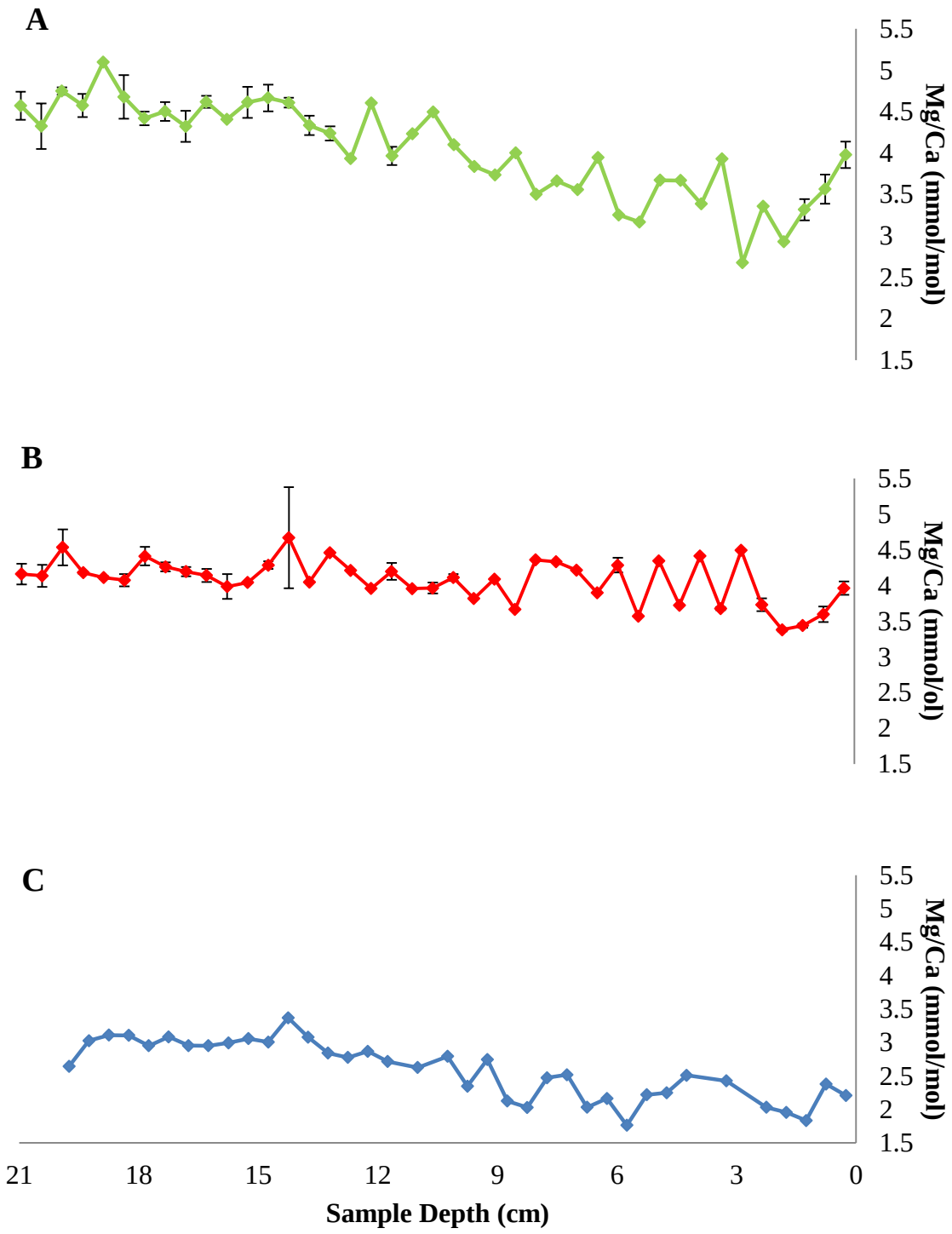

Figure 5: Raw Mg/Ca plotted against core depth for (A) *G. ruber* (white) (B) *G. ruber* (pink) (C) *Gl. truncatulinoides* (non-encrusted). Error bars represent environmental error between replicated samples.

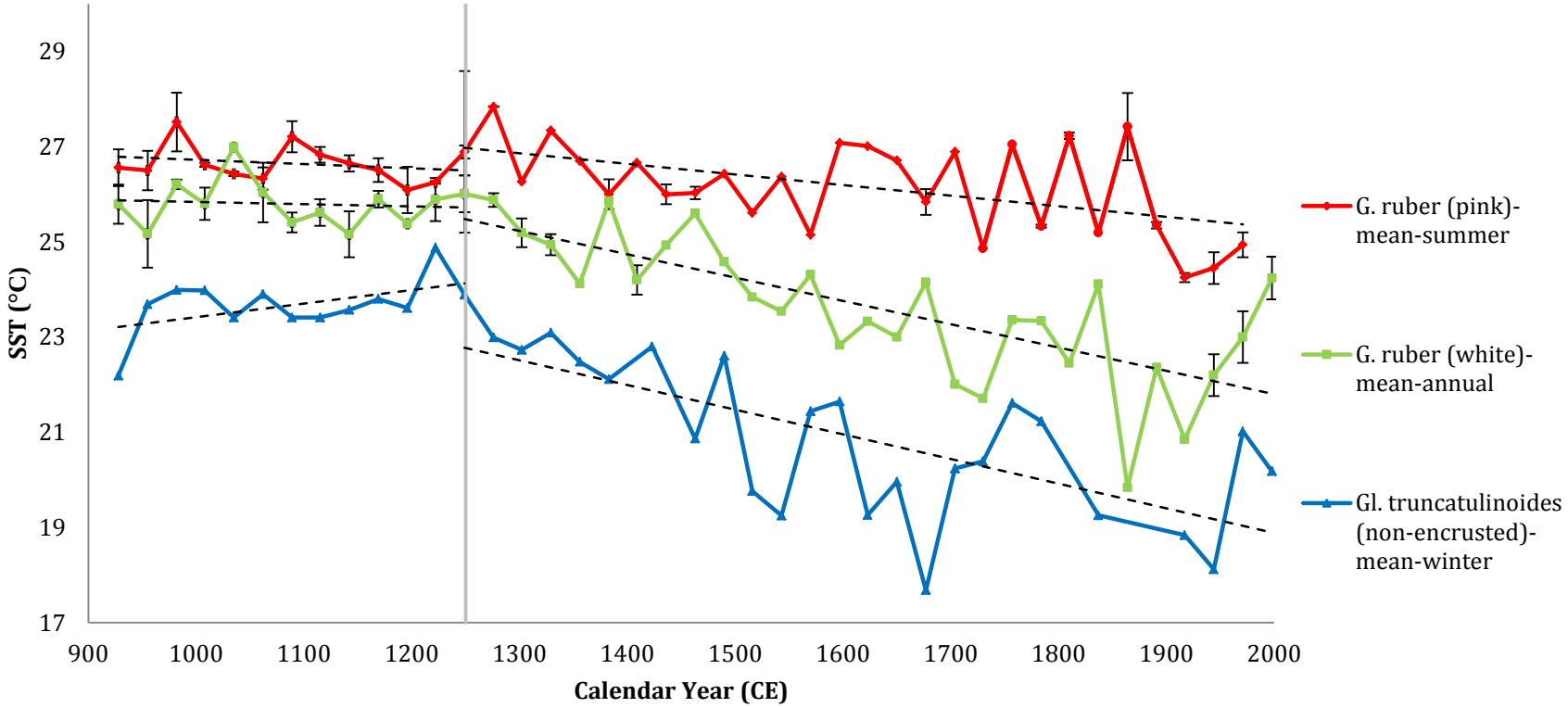

Figure 6: Mean seasonal (summer and winter) and mean-annual Mg/Ca data. Error bars represent environmental error between replicated samples. Gray line represents 1250 CE. Dashed lines represent trends from 900 to 1250 CE and 1250 to 2000 CE.

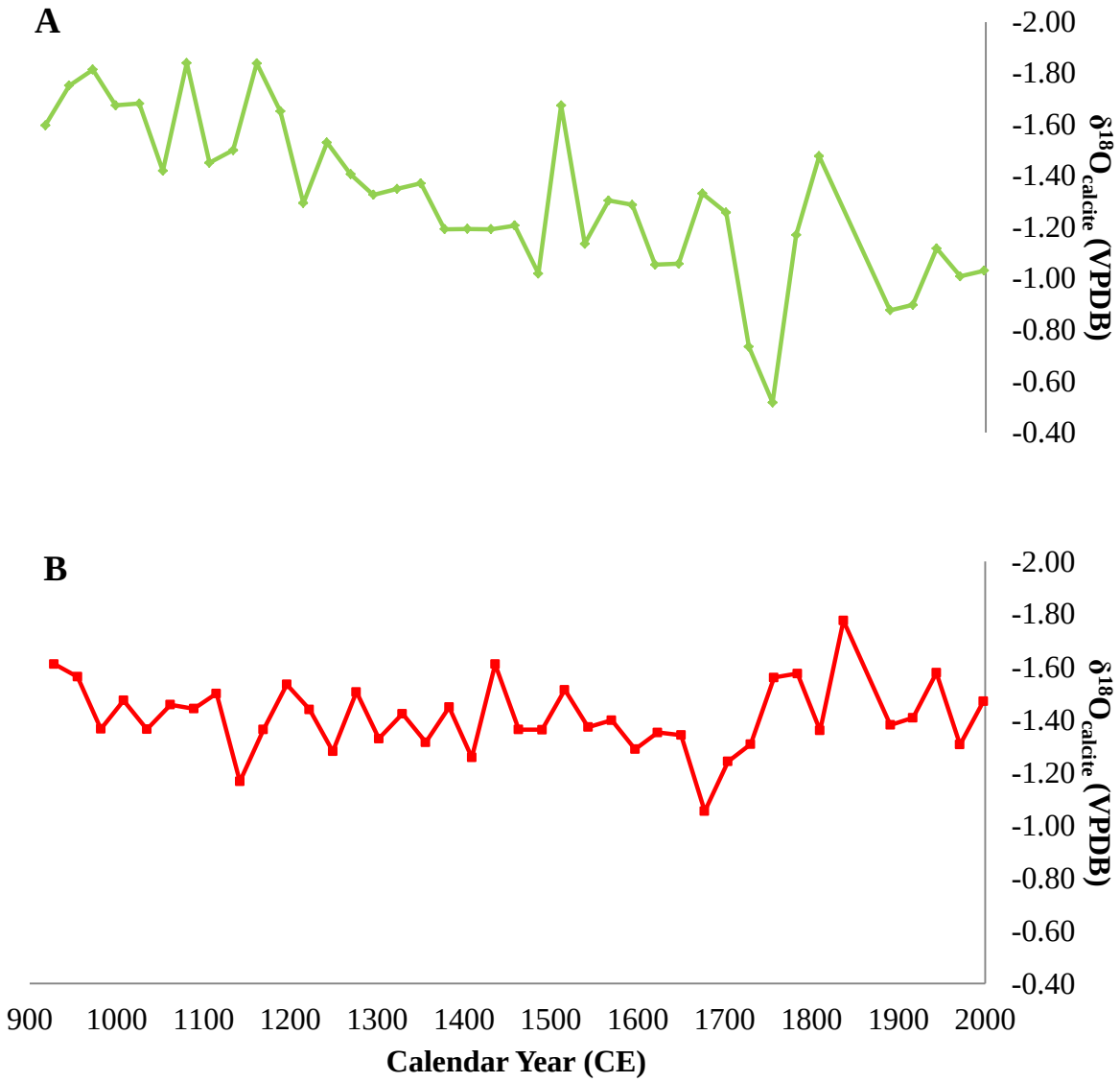

Figure 7: Raw $\delta^{18}O_{calcite}$ (VPDB) for (A) *G. ruber* (white) and (B) *G. ruber* (pink).

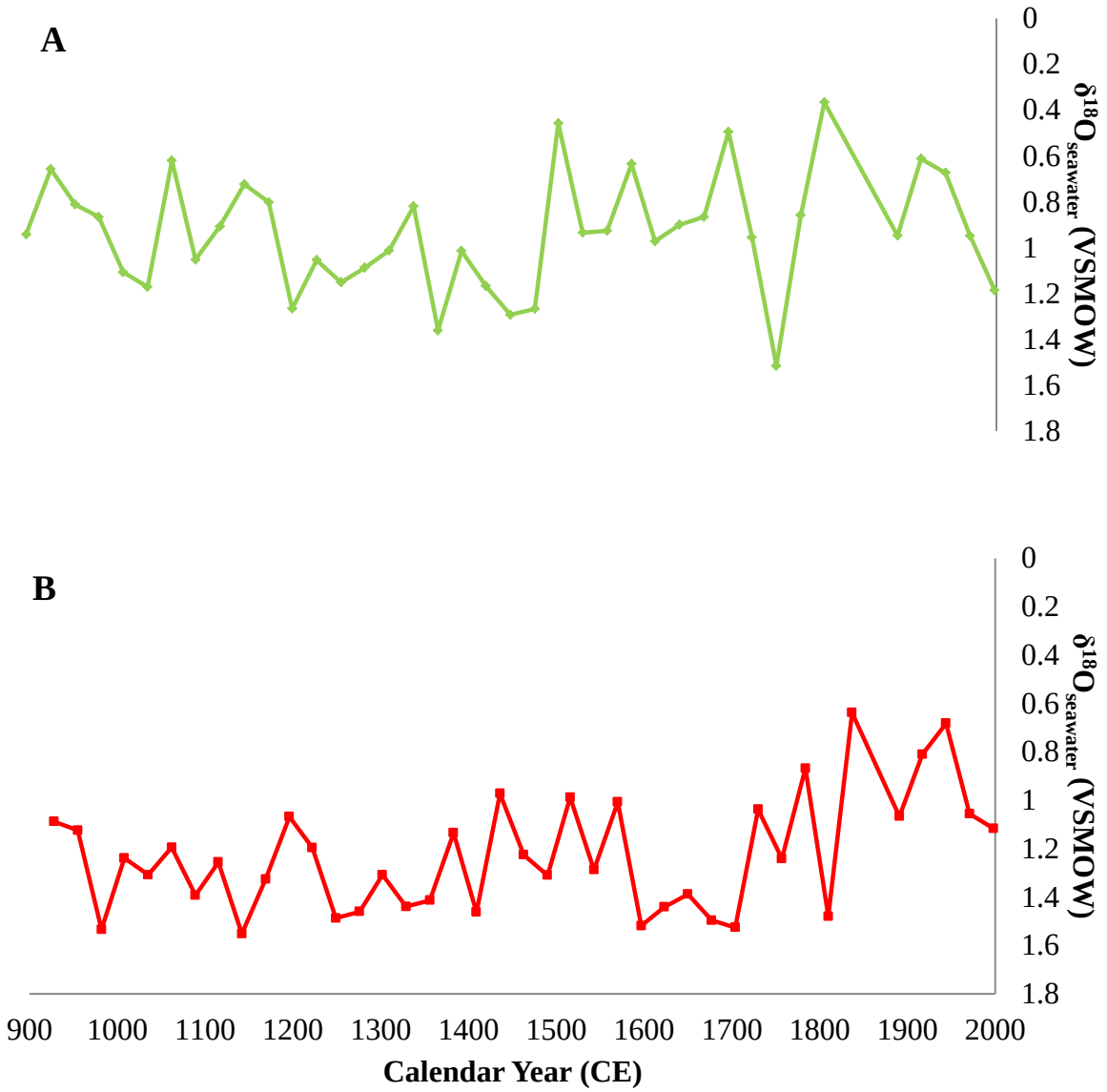

Figure 8: Calculated $\delta^{18}O_{seawater}$ for (A) *G. ruber* (white) and (B) *G. ruber* (pink) based on paired Mg/Ca SST estimates and $\delta^{18}O_{calcite}$ using the *Orbulina universa* high-light equation [SST(ºC) = 14.9-4.8(δc – δw)] (Bemis et al., 1998). Resulting $\delta^{18}O_{seawater}$ was converted from Vienna Peedee belemnite to Vienna standard mean ocean water (VSMOW) by adding 0.27‰.

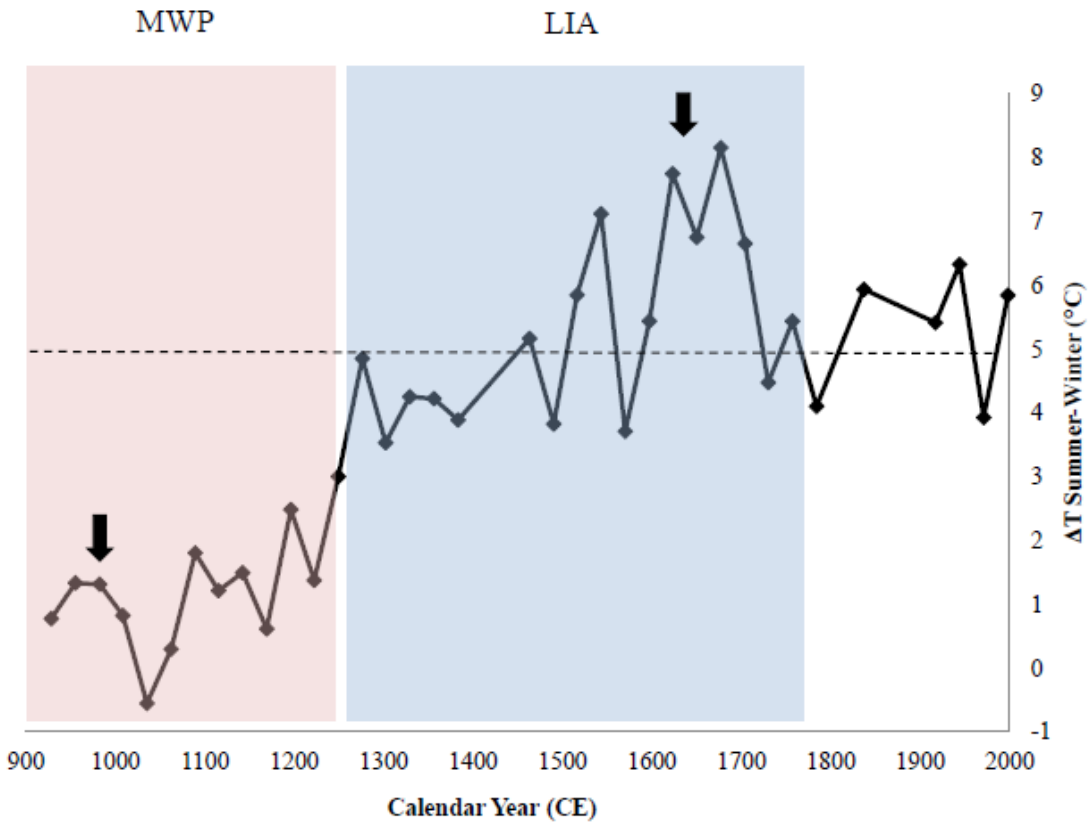

Figure 9: The difference between summer (April-October) and winter (December-February) SST. The dashed line represents modern summer-winter SST (~5ºC) based on the National Oceanographic Data Center World Ocean Atlas 1994. The black arrows show maximum summer SST ca. 980 CE and minimum winter SST ca. 1680 CE.

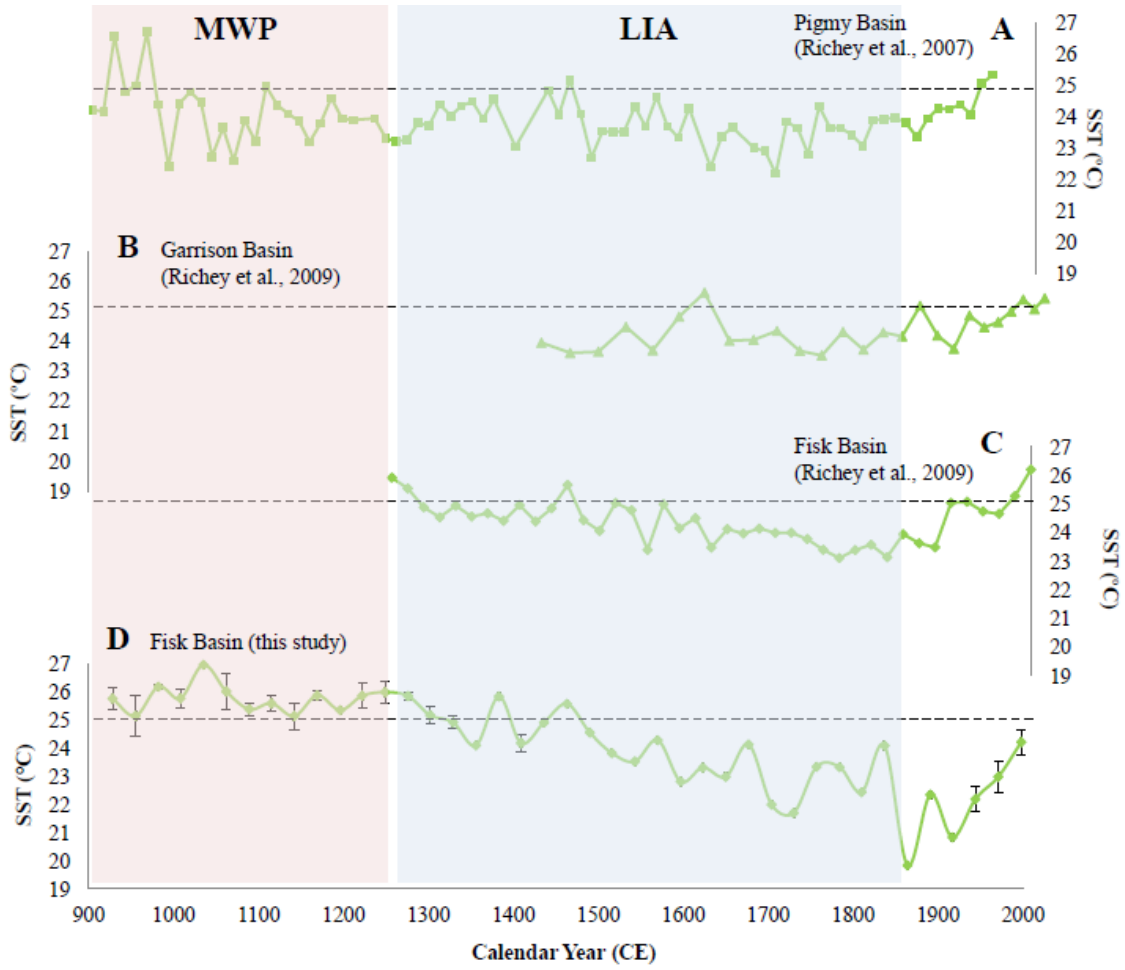

Figure 10: GOM SST data comparison with (A) Pigmy Basin (Richey et al., 2007); (B) Garrison Basin (Richey et al., 2009); and (C) Fisk Basin (Richey et al., 2009). All data are based on *G. ruber* (white) Mg/Ca calibrated to SST using the equation: Mg/Ca = [0.449 × exp (0.09 · SST)] (Anand et al., 2003). Dashed lines represent modern mean-annual SST of 25.4ºC (Leviticus, 2003).

LITERATURE CITED

Anand, P., Elderfield, H., Conte, M.H., 2003. Calibration of Mg/Ca thermometry in planktonic foraminifera from a sediment trap time series. *Paleoceanography* 18(2), 1050. doi:10.1029/2002PA000846

Arbuszewski, J., deMenocal, P., Kaplan, A., Farmer, E.C., 2010. On the fidelity of shell derived $\delta^{18}O_{seawater}$ estimates. *Earth and Planetary Science Letters* 300, 185-196. doi:10.1016/j.epsl.2010.10.035

Barker, S., Greaves, M., Elderfield, H., 2003. A study of cleaning procedures used for foraminiferal Mg/Ca paleothermometry. *Geochemistry, Geophysics, Geosystems* 4(9), 8407. doi: 10.1029/2003GC000559.

Bé A.W.H., Hamlin, W.H., 1967. Ecology of Recent Planktonic Foraminifera: Part 3: Distribution in the North Atlantic during the Summer of 1962. *Micropaleontology* 13(1), 87-106.

Bemis, B.E., Spero, H.J., Bijma, J., Lea, D.W., 1998. Reevaluation of the oxygen isotope composition of planktonic foraminifera: Experimental results and revised paleo-temperature equations. *Paleoceanography* 13, 150-160. doi: 10.1029/98PA00070

Bertler, N.A.N., Mayewski, P.A., Carter, L., 2011. Cold Conditions in Antarctica during the Little Ice Age- Implication for abrupt climate change mechanisms. *Earth and Planetary Science Letters* 308(1-2), 41-51. doi: 10.1016/j.epsl.2011.05.021

Bijma, J., Faber Jr., W.F., Hemleben, C., 1990. Temperature and salinity limits for growth and survival of some planktonic foraminifers in laboratory cultures. *Journal of Foraminiferal Research* 20(2), 95-116.

Black, D.E., Abahazi, M.A., Thunell, R.C., Kaplan, A., Tappa, E.J., Peterson, L.C., 2007. An 8-century tropical Atlantic SST record from the Cariaco Basin: Baseline variability, twentieth-century warming, and Atlantic hurricane frequency. *Paleoceanography* 22(4), PA 4204. doi:10.1029/2007PA001427

Bond, G., Showers, W., Cheseby, M., Lotti, R., Almasi, P., deMenocal, P., Priore, P., Cullen, H., Hajdas, I., Bonani, G., 1997. A Pervasive Millennial-Scale Cycle in North Atlantic Holocene and Glacial Climates. *Science* 278, 1257-1266.

Bond, G., Kromer, B., Beer, J., Muscheler, R., Evans, M.N., Showers, W., Hoffmann, S., Lotti-Bond, R., Hajdas, I., Bonani, G., 2001. Persistent solar influence on North Atlantic climate during the Holocene. *Science* 294(5549), 2130-2136.

Bradley, R.S., Hughes, M.K., Diaz, H., 2003. Climate in Medieval Time. *Science* 302(5644), 404-405. doi:10.1126/science.1090372

Broecker, W.S., 2001. Was the Medieval Warm Period Global? *Science* 291(5508), 1497-1499.

Cane, M.S., 2010. Decadal predictions in demand. *Nature Geoscience* 3(4), 231-232. doi:10.1038/ngeo823

Chave, K.E., 1954. Aspects of the biogeochemistry of magnesium: calcareous marine organisms. *Journal of Geology* 62(3), 266-283.

Crowley, T., 2000. Causes of Climate Changes Over the Past 1000 Years. *Science* 289(5477), 270-277. doi: 10.1126/science.289.5477.270

Dekens, P.S., Lea, D.W., Pak, D.K., Spero, H.J., 2002. Core top calibration of Mg/Ca in tropical foraminifera: refining paleotemperature estimation. *Geochemistry Geophysics, Geosystems* 3(4). 1-29. doi: 10.1029/2001GC000200

deMenocal. P., Oritz, J., Guilderson, T., Sarnthein, M., 2000. Coherent High- and Low-Latitude Climate Variability During the Holocene Warm Period. *Science* 288(5474), 2198-2202. doi: 10.1126/science.288.5474.2198

Deuser, W.G., Ross, E.H., 1989. Seasonally abundant planktonic foraminifera of the Sargasso Sea: Succession, deep-water fluxes, isotopic compositions, and paleoceanographic implications. *Journal of Foraminiferal Research* 19(4), 268-293.

Dowsett, H.J., Verardo, S., Poore,R.Z. 2003. Gulf of Mexico planktic foraminifer transfer function GOM2: preliminary report. U.S. Geological Survey Open File Report OF 03-61.

Dowsett, H.J., 2007. Planktic Foraminifera. *Paleoceanography Biological Proxies* 1678-1682.

Esper, J., Schweingruber, F.H., Winiger, M., 2002. 1300 years of climatic history for Western Central Asia inferred from tree-rings. *The Holocene* 12(3), 267-277. doi: 10.1191/0959683602hl543rp

Ferguson, J.E., Henderson, G.M., Kucera, M., Rickaby, R.E.M., 2008.Systematic change of foraminiferal Mg/Ca ratios across a strong salinity gradient. *Earth and Planetary Science Letters* 265, 153-166. doi:10.1016/j.epsl.2007.10.011

Hasse-Schramm, A., F. Böhm, A. Eisenhauer, W.-C. Dullo, M. M.Joachimski, B. Hansen, and J. Reitner., 2003. Sr/Ca ratios and oxygen isotopes from scelrosponges: Temperature history of the Caribbean mixed layer and thermocline during the Little Ice Age, Paleoceanography 18(3), 1073, doi: 10.1029/2002PA000830

Helama, S., Seppä, H., Birks, J.B., Bjune, A.E., 2010. Reconciling pollen-stratigraphical and tree-ring evidence for high- and low- frequency temperature variability in the past millennium. *Quaternary Science Reviews* 29(27-28), 3905-3918. doi: 10.1016/j.quascirev.2010.09.012

Hemleben, C., Spindler, M., Breitinger, I., Deuser, W.G., 1985. Field and laboratory studies on the ontogeny and ecology of some globorotaliid species from the Sargasso Sea off Bermuda. *Journal of Foraminiferal Research* 15(4), 254–272.

Jones, P.D., Osborn, T.J., Briffa, K.R., 2001. The Evolution of Climate Over the Last Millennium. *Science* 292(5517), 662-667. doi: 10.1126/science.1059126

Kilbourne, K.H., Quinn, T.M., Webb, R., Guilderson, T., Nyberg, J., Winter, A., 2008. Paleoclimate proxy perspective on Caribbean climate since the year 1751: Evidence of cooler temperatures and multidecadal variability. *Paleoceanography* 23(3), PA3220. doi:10.1029/2008PA001598

Kisakurek, B., Eisenhauer, A., Bohm, F., Garbe-Shonberg, D., Erez, J., 2008.Controls on shell Mg/Ca and Sr/Ca in cultured planktonic foraminiferan *Globigerinoides ruber* (white). *Earth and Planetary Science Letters* 273, 260-269. doi:10.1016/j.epsl.2008.06.026

Kreutz, K.J., Mayewski, P.A., Meeker, L.D., Twickler, M.S., Whitlow, S.I., Pittalwala, I.I., 1997. Bipolar changes in atmospheric circulation during the Little Ice Age. *Science* 277(5330), 1294-1296.

Lamb, H. H., 1995. Climate, history, and the modern world, 2nd Edition. Routledge.

Levitus, S., 2003. National Oceanographic Data Center World Ocean Atlas 1994, at http://www.cdc.noaa.gov/, Climate Data Center, Boulder, Colorado.

LoDico, J.M., Flower, B.P., Quinn, T.M., 2006. Subcentennial-scale climate and hydrologic variability in the Gulf of Mexico during the early Holocene. *Paleoceanography* 21(3), PA3015. doi: 10.1029/2005PA001243

Luterbacher, J., Dietrich, D., Xoplaki, E., Grosjean,M., Wanner, H., 2004. European seasonal and annual temperature variability, trends, and extremes since 1500. Science 303, 1499-1503. doi: 10.1126/science.1093877

Mann, M.E., Zhang, Z., Rutherford, S., Bradley, R.S., Hughes, M.K., Shindell, D., Ammann, C., Faluvegi, G., Ni, F., 2009. Global signatures and dynamical origins of the Little Ice Age and Medieval Climate Anomaly. *Science* 326(5957), 1256-1260. doi: 10.1126/science.1177303

McKenna, V.S., Prell, W.L., 2004. Calibration of the Mg/Ca of *Globorotalia truncatulinoides* (R) for the reconstruction of marine temperature gradients. *Paleoceanography* 19(2), PA2006. doi: 10.1029/2000PA000604

Moberg, A., Sonechkin, D.M., Holmgren, K., Datsenko, N.M., and Karlén, W., 2005. Highly variable Northern Hemisphere temperatures reconstructed from low- and high-resolution proxy data. *Nature* 433, 613-617. doi: 10.1038/nature03265

Newton, A., Thunnel, R., Stott, L., 2006. Climate and hydrographic variability in the Indo-Pacific Warm Pool during the last millennium. *Geophysical Research Letters* 33(19), L19710. doi: 10.1029/2006GL027234

Nürnberg, D., Bijma, J., Hemleben, C., 1996. Assessing the reliability of magnesium in foraminiferal calcite as a proxy for water mass temperatures. *Geochimica et Cosmochimica Acta* 60(5), 803-814. PII: 0016-7037(95)00446-7

Nürnberg, D., Ziegler, M., Karas, C., Tiedemann, R., Schmidt, M.W., 2008. Interacting Loop Current variability and Mississippi River discharge over the past 400 kyr. *Earth and Planetary Science Letters* 272, 278-289. doi:10.1016/j.epsl.2008.04.051

Oppo, D.W., Rosenthal, Y., Linsley, B.K., 2009. 2,000-year-long temperature and hydrology reconstructions from the Indo-Pacific warm pool. *Nature* 460(7259), 1113-1116. doi: 10.1038/nature08233

Pinet, Paul R., 2009. Invitation to Oceanography, 5th Edition.Jones and Barlett Publishers, LLC. p. 118.

Poore, R.Z., Quinn, T.M., Verardo, S., 2004. Century-scale movement of the Atlantic Intertropical Convergence Zone linked to solar variability. *Geophysical Research Letters* 31(12), L12214. doi: 10.1029/2004GL019940

Poore, R.Z., 2008. Holocene climate and climate variability of the northern Gulf of Mexico and adjacent northern Gulf Coast: A review. The Open Paleontology Journal 1, 7-17.

Reimer, P.J., Baillie, M.G.L., Bard, E., Bayliss, A., Beck, J.W., Blackwell, P.G., Bronk Ramsey, C., Buck, C.E., Burr, G.S., Edwards, R.L., Friedrich, M., Grootes, P.M., Guilderson, T.P., Hajdas, I., Heaton, T.J., Hogg, A.G., Hughen, K.A., Kaiser,

K.F., Kromer, B., McCormac, F.G., Manning, S.W., Reimer, R.W., Richards, D.A., Southon, J.R., Talamo, S., Turney, C.S.M., van der Plicht, J., Weyhenmeyer, C.E., 2009. INTCAL09 and MARINE09 radiocarbon age calibration curves, 0-50,000 years CAL BP. *Radiocarbon* 51(4), 1111-1150.

Reynolds, C.E., Richey, J.N., Poore, R.Z., 2013. Seasonal flux and assemblage composition of planktic foraminifera from the northern Gulf of Mexico, 2008-2012. U.S.Geological Survey Open File Report 2013-1243.

Richey, J.N., Poore, R.Z., Flower, B.P., Quinn, T.M., 2007. 1400 yr multiproxy record of climate variability from the northern Gulf of Mexico. *Geology* 35(5), 423-426. doi: 10.1130/G23507A.1

Richey, J. N., Poore, R.Z., Flower, B.P., Quinn, T.M., Hollander, D.J., 2009. Regionally coherent Little Ice Age cooling in the Atlantic Warm Pool. *Geophysical Research Letters* 36(21), L21703. doi:10.1029/2009GL040445.

Richey, J.N., Hollander, D.J., Flower, B.P., Eglinton, T.I., 2011. Merging late Holocene molecular organic and foraminiferal-based geochemical records of sea surface temperature in the Gulf of Mexico. *Paleoceanography* 26(1), PA1209. doi: 10.1029/2010PA002000

Richey, J., Poore, R.Z., Flower, B.P., Hollander, D.J., 2012. Ecological controls on the shell geochemistry of pink and white *Globigerinoides ruber* in the northern Gulf of Mexico: Implications for paleoceanographic reconstruction. *Marine Micropaleontology* 82-83 (C), 28-37. doi:10.1016/j.marmicro.2011.10.002

Ruddiman, W.F., 2007. The early anthropogenic hypothesis: challenges and responses. *Reviews of Geophysics*, 45(4), RG4001. doi: 10.1029/2006RG000207

Spear, J.W., Poore, R.Z., Quinn, T.M., 2011. *Globorotalia truncatulinoides* (dextral) Mg/Ca as a proxy for Gulf of Mexico winter mixed-layer temperature: Evidence from a sediment trap in the northern Gulf of Mexico. *Marine Micropaleontology* 80(3-4), 53-61. doi:10.1016/j.marmicro.2011.05.001

Spero, Howard J., 2001. Life History and Stable Isotope Geochemistry of Planktonic Foraminifera. Isotope Paleobiology and Paleoecology: *Paleontological Society Papers* 4, 1-41, Special Publication.

Tolderlund, D.S., Bé, A.W.H., 1971. Seasonal Distribution of Planktonic Foraminifera in the Western North Atlantic. *Micropaleontology* 17(3), 297-329.

Wang, C., Enfield, D.B., 2001. The Western Hemisphere Warm Pool. *Geophysical Research Letters* 28, 1635-1638. doi: 10.1029/2000GL011763

Wang, C., Enfield, D. B., 2003. A Further Study of the Tropical Western Hemisphere Warm Pool. *Journal of Climate* 16, 1476-1493.

Wang, C., Enfield, D.B., Lee, S., Landsea, C.W., 2006. Influences of the Atlantic Warm Pool on Western Hemisphere Summer Rainfall and Atlantic Hurricanes. *Journal of Climate* 19, 3011-3028.

Wang, C., Lee, S., Enfiled, D.B., 2008. Climate Response to Anomalously Large and Small Atlantic Warm Pools during the Summer. *Journal of Climate* 21(11), 2437-2450. doi: 10.1175/2007JCLI2029.1

Wang, C., Liu, H., Lee, S., Atlas, R., 2011. Impact of the Atlantic warm pool on United States landfalling hurricanes. *Geophysical Research Letters* 38(19), L19702. doi: 10.1029/2011GL049265

Wantanabe, T., Winter, A., Oba, T., 2001. Seasonal changes in sea surface temperature and salinity during the Little Ice Age in the Caribbean Sea deduced from Mg/Ca and $^{18}O/^{16}O$ ratio in corals. *Marine Geology* 173, 21-35. PII: S0025-3227(00)00166-3

Wefer, G., Berger, W.H., Bijma, J., Fischer, G., 1999. Clues to Ocean History: a Brief Overview of Proxies. *Scripps Institution of Oceanography* 1-68. Print.

Williams, C., Flower, B.P., Hastings, D.W., Guilderson, T.P., Quinn, K.A., Goddard, E.A., 2010. Deglacial abrupt climate change in the Atlantic Warm Pool: A Gulf of Mexico perspective. *Paleoceanography* 115(4), PA4221. doi: 10.1029/2010PA001928

Winter, A., Ishioroshi, H., Wantanabe, T., Oba, T., Christy, J., 2000. Caribbean sea surface temperatures: two-to-three degrees cooler than present during the Little Ice Age. *Geophysical Research Letters* 27(20), 3365-3368.

Žarić, S., Donner, B., Fischer, G., Mulitza, S., Wefer, G., 2005. Sensitivity of planktic foraminifera to sea surface temperature and export production as derived from sediment trap data. *Marine Micropaleontology* 55, 75-105. doi: 10.1016/j.marmicro.2005.01.002